

An Analysis of High Selectivity and Harmonic Suppression Based on Stepped-Impedance Resonator Structure for Dual-Mode Diplexer

Jessada Konpang¹ and Natchayathorn Wattikornsirikul^{2, *}

Abstract—A high selectivity microstrip dual-mode diplexer with a stepped-impedance opened-end structure is implemented to reduce the size of a dual-mode resonator and suppress the harmonics. The proposed dual-mode resonator structure consists of a microstrip half-wavelength resonator and an open-circuited stepped-impedance stub. The stepped-impedance opened-end structure can control an even mode in the upper and lower desired bands to improve the cutoff responses. The sharp cutoff selectivity of the filter is created to enhance the diplexer performance and wide suppress harmonics. The dual-mode diplexer prototype is analyzed, fabricated, and measured. The measured result agrees well with the analyzed result. The simulated and measured dual-mode diplexers are designed at the operational frequency of Tx/Rx at 1.95 GHz and 2.14 GHz, respectively. It is shown that the dual-mode filter has a wide stopband due to the stepped-impedance stub.

1. INTRODUCTION

Recently, with the development of RF/microwave components and systems, microstrip filters with high-frequency selectivity, compact size, and wide stopband are highly demanded. Several structures of dual-mode microstrip filters with perturbation elements have been used, including dual-mode ring resonator [1], square-ring resonator based on coplanar waveguide (CPW) structure [2], and multi-arc resonator filter with four identical semicircular [3]. As mentioned above, geometrically symmetrical resonators of a dual-mode filter have two degenerate resonant modes introduced by a perturbation element in a resonator. Subsequently, a microstrip dual-mode open-loop resonator has been presented [4]. This type of open-loop dual-mode resonator by loading part inside the open-loop does not affect the odd mode characteristic.

Nevertheless, filter and diplexer resonator with high-frequency selectivity, compact size, and wide stopband are still prime considerations to be improved for communication systems. A microstrip resonator with internal coupled lines and an open-circuited stub is presented in [5]. After that, many researchers have proposed various kinds of dual-mode microstrip resonator configurations for bandpass filter designs [6]. A high cutoff selectivity dual-mode filter can be controlled by adjusting the open-circuited stub. However, this microstrip filter has a large size. It is difficult to suppress harmonic on the upper sideband, which will degrade the filter and diplexer circuits' passband performance.

The filter applications are used for transmitting (Tx) and receiving (Rx) channels in diplexer RF front-end circuits. A diplexer is a three-port component that it commonly consists of two bandpass filters with different resonant frequencies. To achieve a diplexer design with good frequency selectivity, improve out of band rejection, and reduce interference between the adjacent channels, transmission

Received 21 March 2021, Accepted 14 April 2021, Scheduled 19 April 2021

* Corresponding author: Natchayathorn Wattikornsirikul (natchayathorn.w@rmutp.ac.th).

¹ Department of Electronics and Telecommunication Engineering, Faculty of Engineering, Rajamangala University of Technology Krungthep, 2 Nanglingee Rd., Thungmahamek, Sathorn, Bangkok 10120, Thailand. ² Department of Electronic and Telecommunication Engineering, Faculty of Engineering, Rajamangala University of Technology Phra Nakhon, 131 Pracharat 1 Rd., Wongsawang, Bang Sue, Bangkok 10800, Thailand.

zeros (TZs) and high signal isolation are usually the aim in diplexer design. Typically, TZs are helpful for improving the isolation for more superior performance. TZs can be typically realized by coupling structures such as cross-coupling.

Besides designing diplexers with good signal in the band, and high signal isolation out of the band is still stringent to achieve this response. The signal transmitting power can leak between the transmitting and receiving channels when the high power transmitting signal is sent out and interferes the Rx channel. Various research works have been widely presented to increase the diplexer isolation while keeping an easy construction. Many different filters and diplexers have been proposed to increase the signal isolation in diplexer [7–16], which are based on the open-loop single-mode resonator filter structure [7]. Square open loop with stepped impedance resonators can be realized in [8]. A T-shaped resonator and a stub loaded resonator are proposed in [9, 10]. Dual-mode and hybrid resonators are implemented in [11–13]. Varieties of filters and diplexers are mentioned in many material designs such as quarter-wavelength resonator filter [14], filter and diplexer with mixed electromagnetic coupling [15], and Low-temperature co-fired ceramic (LTCC) diplexer using a common stub-loaded resonator [16]. Generally, when high signal isolation is required, a high-order resonator filter is needed, leading to a more complicated circuit. Another way to achieve high signal isolation is a four-port network [17]. However, this technique is still complex in structure and large circuits.

Moreover, to implement metamaterials with microstrip transmission lines, composite right/left-handed (CRLH) transmission lines are proposed [18–22]. There are different types of CRLH transmission lines that can be realized, including interdigital and complementary split-ring resonator (CSRR) [18] and triplexer [19]. CRLH transmission lines can be utilized in active components, namely distributed amplifiers [20]. CRLH transmission lines can be potentially employed in a wide variety of passive components such as filters [21]. To implement metamaterials with microstrip transmission lines, composite right/left-handed (CRLH) transmission lines [22] and coupler [23] are proposed. Due to the requirement of unwanted power signals from the transmitter leak to the receiver, an alternative solution is the asymmetric filter response technique that is easy and not complicated.

This paper presents the easy flexibility of a dual-mode diplexer using a stepped impedance stub with high isolation and a wide stopband based on a controllable TZs technique and stepped-impedance structure. Both high signal isolation and upperside wide stopband can be represented to improve the in-band frequency responses. The proposed dual-mode structure also has a compact size and wide-suppress harmonics due to the stepped-impedance resonator's characteristic responses, controlling the resonant or extending the second harmonics

2. DUAL-MODE TWO-POLE RESONATOR FILTER ANALYSIS

The dual-mode filter structure in [24] is used as the basic configuration of this proposed technique. The dual-mode resonator typically has an even mode resonance which acts as a second-order filter response. The schematic dual-mode filter is presented in Fig. 1. The folded stepped-open stub is connected at the midpoint of a conventional microstrip half-wavelength resonator for tuning the even mode to the odd mode. The extended open-ended stub explained in [24] can be adjusted easily to move the even mode while the odd mode is fixed at the center frequency.

The proposed dual-mode resonator structure consists of a microstrip half-wavelength resonator with an open circuited stepped-impedance stub, illustrated in Fig. 1. Due to the symmetrical resonator

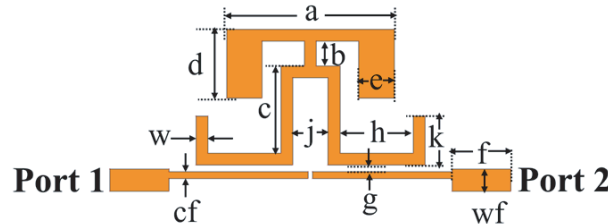


Figure 1. Geometry structure of dual-mode folded stepped-impedance opened-end.

structure, the classical method's use analyzes even and odd-mode excitation resonant conditions. The stepped-impedance is the simplest type of microstrip from a theoretical perspective to reduce the size circuit and suppress harmonic for the basic microwave half-wavelength resonator filter.

The represented equivalent circuits of even and odd modes are shown in Fig. 2. The even mode resonator is presented as an open-circuited structure which is referred to as a half-wavelength resonator as in Fig. 2(a). In contrast, the odd mode resonator is referred to as a short-circuited structure (quarter-wavelength resonator) and is expressed as in Fig. 2(b), where $Z_1, \theta_1, Z_2, \theta_2, Z_3,$ and θ_3 stand for the characteristic impedances and electric lengths of the microstrip stepped-impedance line and open strip impedance stub, respectively.

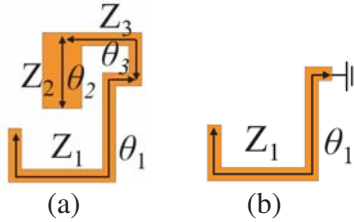


Figure 2. Equivalent circuits of (a) even-mode resonator, (b) odd-mode resonator.

The proposed structure of a dual-mode resonator with folded open-end stub improves the overall size and flexible structure. Moreover, dual-mode performance can also be employed to achieve the filter responses in [24]. The two different sections of the main resonator and folded resonator impedances are shown in Fig. 2. The electrical lengths could be calculated as the following equations

$$\theta_1 \cong \pi/2 \tag{1}$$

The folded-open stub with different impedances (Z_2, Z_3) connects to the resonator's middle (Z_1), where Z_2 and Z_3 represent the even mode equivalent impedances of the folded-open stub sections. Let $R = Z_3/Z_2$, so $R > 1$ for the stepped impedance resonator where $Z_3 > Z_2$. Impedance Z_2 has the electrical length (θ_2) which is presented as

$$\theta_2 = \cos^{-1} \left(\sqrt{\frac{R(R-1)}{(R^2-1)}} \right) \tag{2}$$

Z_3 has the electrical length (θ_3) for the impedance, which is replaced as an open-circuited stub.

$$\theta_3 \cong (\pi + a \tan [-R \tan (\theta_2)]) - \left(\frac{c}{4f_{odd}} \sqrt{\varepsilon_{eff}} \right) \tag{3}$$

where the speed of light in a vacuum is c .

The dual-mode filter uses IE3D full-wave EM simulations to study its resonance properties. An RT/Duroid substrate having a thickness $h = 1.27$ mm with relative dielectric constant $\varepsilon_r = 6.15$ is used to construct the filters. The feeding ports are coupled to a resonator structure with a line width of conductor strip (cf), and the gap between the feed and the resonator is referred to as g . Two input/output microstrip feeds taken as 50Ω characteristic impedance are utilized for a coupled feed of the proposed dual-mode stepped stub loaded resonator.

The current distributions on the metallic surface for the even- and odd-modes are shown in Fig. 3. These distributions can be easily explained that for the even mode, the location of the adjusted open-stepped impedance stub has the maxima electric field which mainly distributes as shown in Fig. 3(a). Thus, the even mode's resonant frequency shifts with changing the open-stepped impedance stub's values (d). On the contrary, the size of the open-end stepped impedance stub is a virtual ground for the odd mode and does not affect the odd-mode characteristic, including its resonant frequency as shown in Fig. 3(b). From the geometric structure in Fig. 1, the relationship between the resonant frequencies of the two modes splitting and different exciting sizes of stepped open circuit stub loaded for five different values of (d) are varied in Fig. 4.

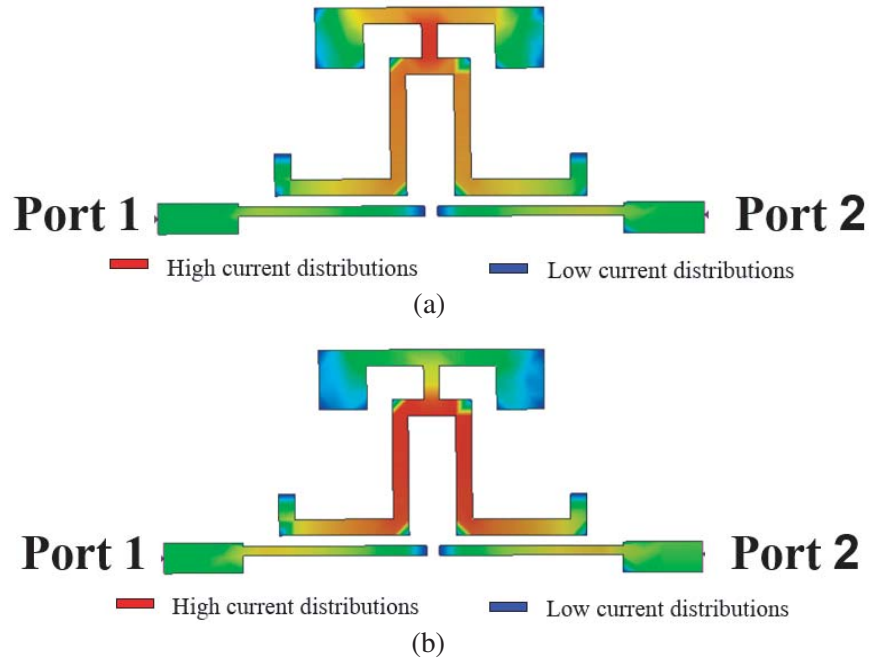


Figure 3. (a) Current distribution of even-mode. (b) Current distribution of odd-mode.

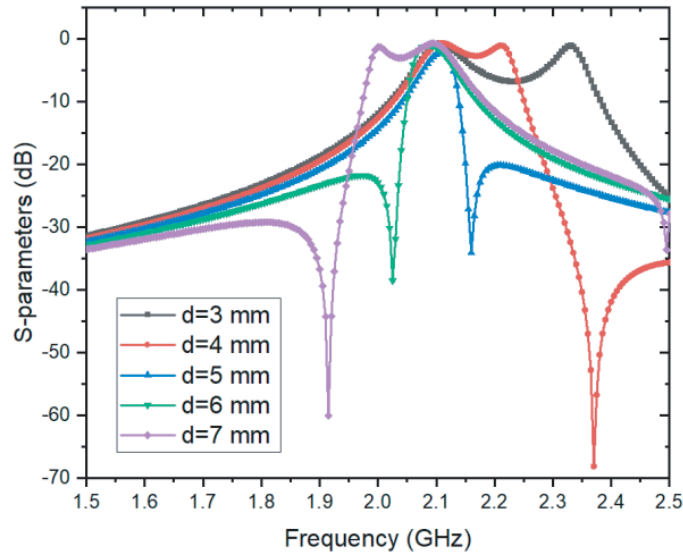


Figure 4. The simulated frequency of different TZs location by changing the length of the stepped open stub.

The relationship between the resonant frequencies of the mode splitting and different perturbation open-stepped impedance lengths (d) is shown in Fig. 4. It can be seen that the stepped open-stub loaded length does not affect the S_{21} response at the odd-mode resonant frequency, and only the second mode resonant frequency is affected in all the cases, while the first one is hardly changed. It can be seen that the mode whose resonant frequency is affected is even, whereas the unaffected mode is odd. The TZs can achieve better performance due to an asymmetric response.

An example of an asymmetric frequency response is designed at the center frequency of 2.14 GHz with 3-dB bandwidth of 60 MHz ($\text{FBW} = 2.8\%$ at 2.14 GHz). The passband insertion loss (IL) is less

than 0.6 dB. The return loss (RL) is better than 20 dB in the passband. The simulated results are plotted in Figs. 5(a) and 5(b). Compared with the traditional dual-mode resonator filter, the proposed microstrip stepped-impedance presents a broad harmonic suppression shown in Fig. 5(c). Fig. 5(c) shows the wideband response compared with the conventional dual-mode resonator structure [17]. The stepped-impedance resonators are compact due to the slow-wave effect and have a wider upper stopband resulting from the dispersion effect. The filter has a wide upper stopband in which a rejection level is kept lower than 25 dB from 2.2 GHz to 4.25 GHz.

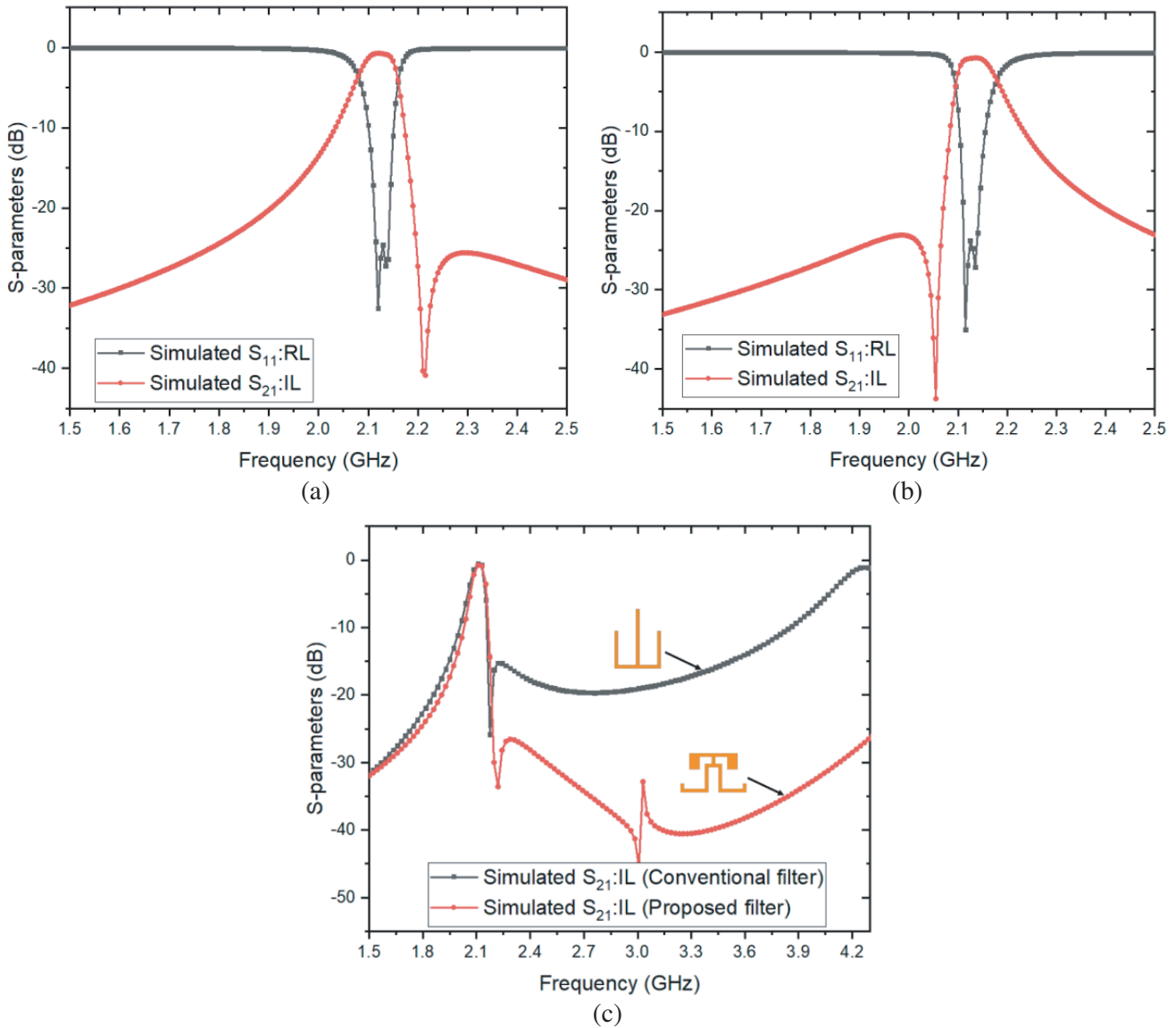


Figure 5. Simulated and measured S -parameters. (a) With transmission zero at the higher passband region. (b) With transmission zero at, the lower passband region. (c) Wideband response of insertion loss compared to the conventional dual-mode filter [17].

3. DUAL-MODE DIPLEXER DESIGN WITH THE UPPER SIDEBAND AT THE CENTER FREQUENCY OF (1.95 GHZ) AND LOWER THE CENTER FREQUENCY OF (2.14 GHZ)

A compact dual-mode resonator enables the ease of asymmetrical frequency response. The diplexer design requires high isolation signal or high attenuation between the transmitter and receiver frequencies. Two back-to-back TZs are combined in the form of a high selectivity diplexer, which helps diplexer performance well. This technique improves the channel performance between the Tx and Rx frequency bands, and stepped impedance resonators are easily employed to construct the proposed device, combined with a high-performance dual-mode diplexer.

A two-pole dual-mode resonator filter structure with proximity coupling gaps was individually designed for each filter channel. The diplexer design is based on the independent design of two dual-mode filters as in following steps.

The first step: filter is designed at 1.95 GHz with upper sideband TZ and 60 MHz bandwidth in Tx between ports 1 and 2.

The second step: dual-mode filter has a resonant frequency at 2.14 GHz and 60 MHz bandwidth in

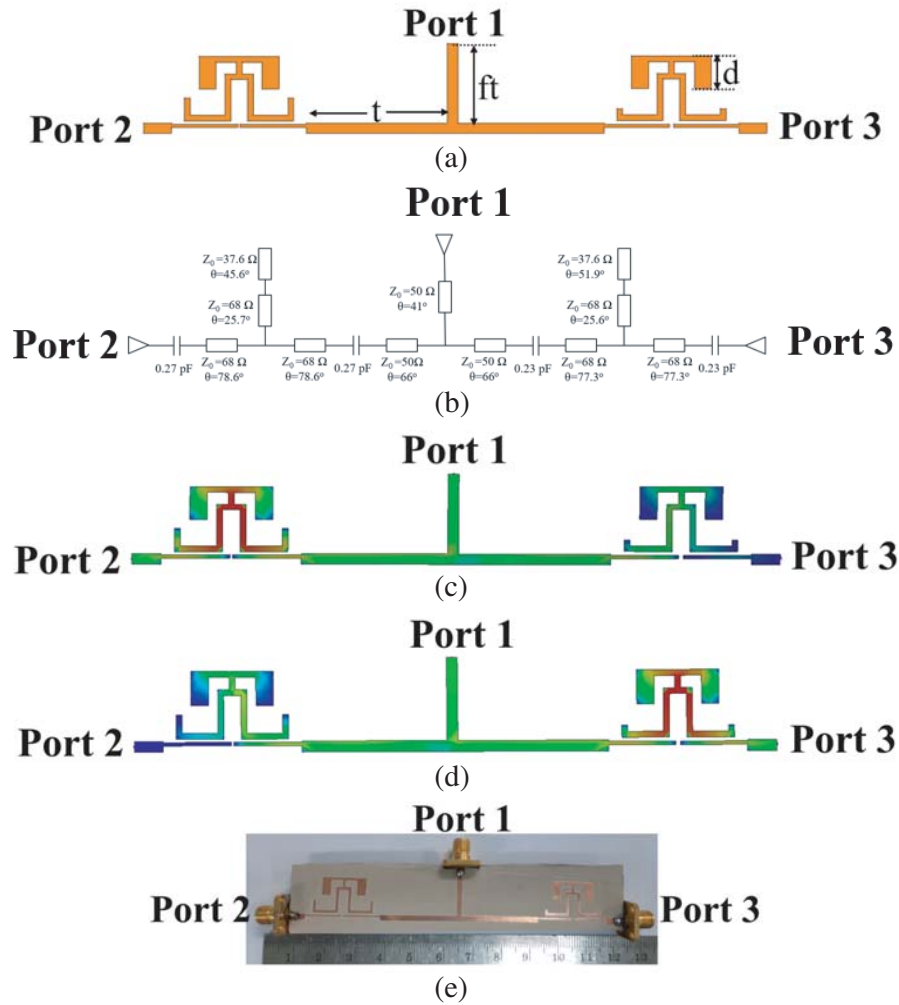


Figure 6. (a) Geometric structure. (b) Equivalent circuit of the transmission line. (c) Distributed current flows of the diplexer at low passband state (1.95 GHz). (d) High passband state at 2.14 GHz. (e) The layout of a fabricated prototype of diplexer with TZ at the higher stopband region (1.95 GHz) and with transmission zero at the lower stopband region (2.14 GHz).

Tx between ports 1 and 2. This resonant filter is designed with a transmission zero at the lower-sideband of the center frequency.

Final step: two dual-mode filters are combined via transmission-line-based T-junctions with a coupling line in the form of a three-port diplexer.

The geometry and dimensions have been proved to obtain good impedance matching by simulation and optimization. The proposed dual-mode diplexer schematic construction is shown in Fig. 6(a). It is essential to combine the two independent filters with a matching network. T-junction is used to interconnect the two filters using an appropriately designed matching circuit. The proposed dual-mode diplexer keeps the advantages of simple structure, easy machining, low cost, low loss, and miniaturization.

Moreover, the equivalent transmission circuit of dual-mode resonator diplexer is shown in Fig. 6(b). Electromagnetic (EM) simulator IE3D is used to perform the distributed current and S -parameter responses. The distributed current flows on the metallic surface at the center frequency at 1.95 GHz

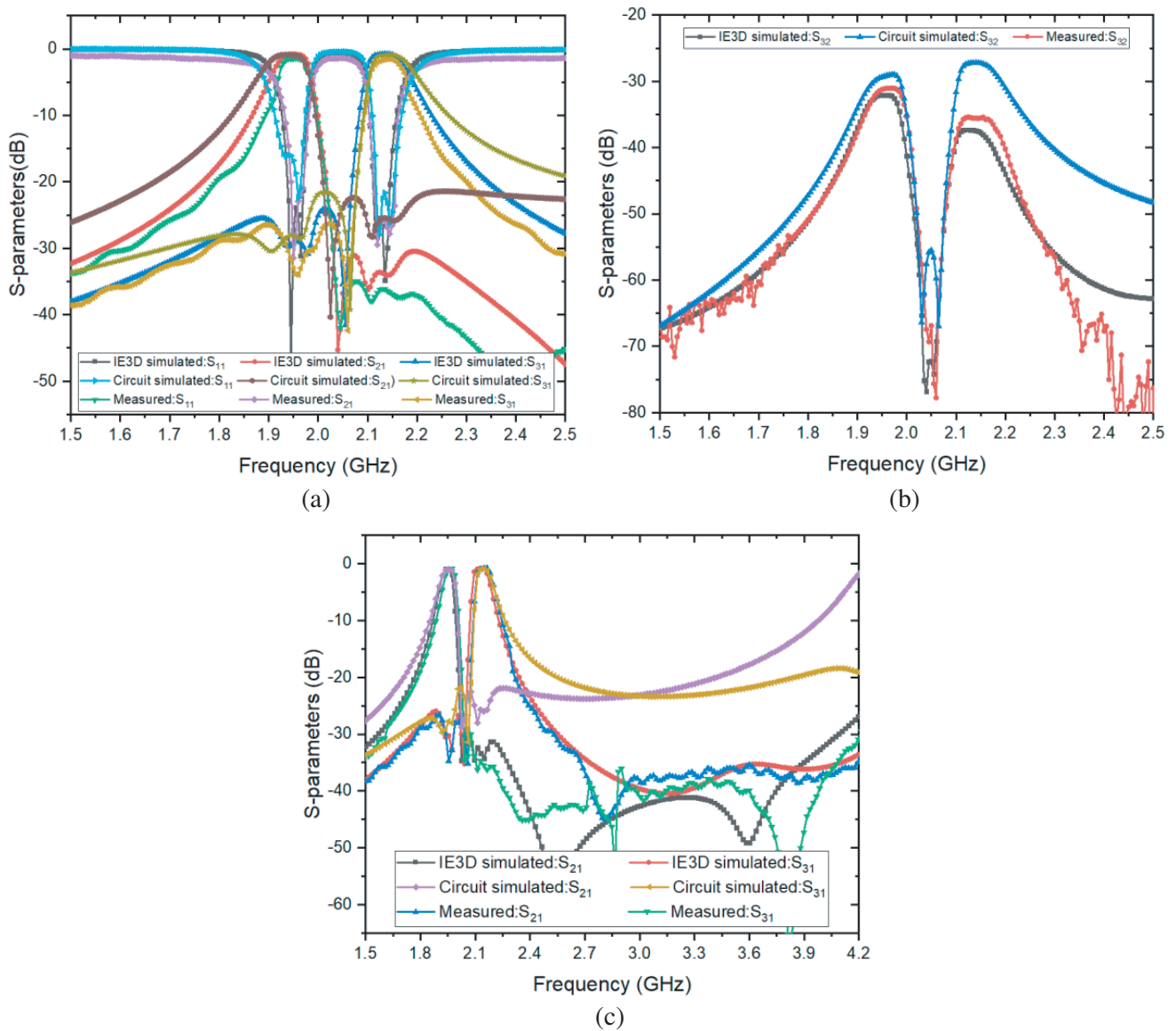


Figure 7. Simulated and measured S -parameters. (a) With transmission zero between two passbands region. (b) Isolation (S_{32}) of dual-mode diplexer. (c) Wideband response of dual-mode diplexer.

Table 1. Schematic dimensions of the proposed dual-mode resonator diplexer.

Dimensions	$R_X = 1.95 \text{ GHz}$	$T_X = 2.14 \text{ GHz}$
Width of the resonator (w)	1 mm	1 mm
Width of the resonator (wf)	1.87 mm	1.87 mm
Width of the resonator (cf)	0.6 mm	0.6 mm
The gap of the resonator (g)	0.55 mm	0.65 mm
Size of the resonator Length (a)	14.2 mm	14.2 mm
Size of the resonator Length (b)	2.1 mm	2.1 mm
Size of the resonator Length (c)	7.4 mm	7.4 mm
Size of the resonator Length (k)	4.1 mm	2.5 mm
Size of the open stub (d)	5.8 mm	5.8 mm
Width of the open stub (e)	3 mm	3 mm
Size of the feed Length (f)	10 mm	10 mm
Length of feed line (ft)	16 mm	16 mm
Length of T-junction feed line (t)	26.6 mm	26 mm

Table 2. Comparison of proposed dual-mode diplexer with the state-of-the-arts diplexer.

References	Types	Degrees	Frequency (GHz)	Insertion loss (dB)	Isolation (dB)	Ports No.
[13]	Dual-mode stub loaded resonator	2	1.95/2.14	1.2/1.5	> 35	3
[14]	Quarter-wavelength resonators	2	1.95/2.14	1.1/1.18	> 40	3
[15]	Mixed electromagnetic coupling	2	2.44/3.52	1.43/1.59	> 42	3
[16]	Low-temperature co-fired ceramic (LTTC)	3	1.95/2.14	1.74/2.37	> 40	3
This work	Dual-mode stepped-impedance resonator	2	1.95/2.14	1.02/1.12	> 32	3

and 2.14 GHz, portrayed in Figs. 6(c) and 6(d), respectively. A photograph of the diplexer prototype is shown in Fig. 6(e). Agilent Vector Network Analyzer is used to measure the proposed dual-mode diplexer prototype. Simulated and measured results of the dual-mode are analyzed under simulator and network analyzer, which show a good agreement. The optimized diplexer geometry dimensions are tabulated in Table 1. Fig. 7(a) shows that the measured insertion losses $/S_{21}, S_{31}/$ in the low passband and high passband channels are 1.02 dB and 1.12 dB, respectively. The isolation (S_{32}) performance reveals the rejection level greater than 32 dB isolation, as shown in Fig. 7(b). A wideband measured result shows a wide suppress harmonic due to stepped-impedance stub. The out-of-band rejection level is kept below 30 dB over the frequency range from 2.5 to 4.2 GHz, as shown in Fig. 7(c).

Meanwhile, a good agreement between the measured and simulated results has been achieved. The figures indicate that the proposed dual-mode diplexer exhibits a sharp cutoff response. The measured

s-parameters prove that the dual-mode diplexer shows good insertion loss and return loss and good agreement with the simulated results. Due to the SMA connectors and fabricated process errors, the extra losses in the measured S -parameters are believed to occur.

Table 2 shows the comparison of several three-port diplexers and the proposed dual-mode diplexer. It can be seen that the proposed dual-mode diplexer exhibits good in-band performance and high isolation.

4. CONCLUSIONS

A compact and simple dual-mode structure with asymmetrical frequency response control attenuation between the transmitter and receiver frequencies is proposed for diplexer design. High signal isolation and wide stopband based on controllable TZs technique are proposed here. Both high signal isolation and upper-side wide stopband can be represented to improve the in-band frequency responses. Furthermore, the high signal isolation is achieved using even-odd mode and transmission zero control at the higher stopband region (1.95 GHz) and lower stopband region (2.14 GHz). The stepped-impedance resonators are compact due to the slow-wave effect, but they also have a wider upper stopband resulting from the dispersion effect.

ACKNOWLEDGMENT

Thanks to the Department of Electronic and Telecommunication Engineering, Faculty of Engineering, Rajamangala University of Technology Phranakhon and Department of Electronic and Telecommunication Engineering, Faculty of Engineering, Rajamangala University of Technology Krungthep to support the research successfully.

REFERENCES

1. Tan, B. T., J. J. Yu, S. T. Chew, M.-S. Leong, and B.-L. Ooi, "A miniaturized dual-mode bandpass filter with a new perturbation," *IEEE Microwave and Wireless Components Letter*, Vol. 53, No. 1, 343–345, Jan. 2005.
2. Huang, X. D. and C. H. Cheng, "A novel coplanar-waveguide bandpass filter using a dual-mode square-ring resonator," *IEEE Microwave and Wireless Components Letter*, Vol. 16, No. 1, 13–15, Jan. 2006.
3. Kang, W., W. Hong, and J.Y. Zhou, "Performance improvement and size reduction of microstrip dual-mode bandpass filter," *Electronics Letter*, Vol. 44, No. 6, 421–422, Mar. 2008.
4. Hong, J.-S., H. Shaman, and Y.-H. Chun, "Dual-mode microstrip open-loop resonators and filters," *IEEE Transactions on Microwave Theory and Techniques*, Vol. 55, No. 8, 1764–1770, Aug. 2007.
5. Hua, C., C. Chen, C. Miao, and W. Wu, "Microstrip bandpass filters using dual-mode resonators with internal coupled lines," *Progress In Electromagnetics Research*, Vol. 21, 99–111, 2011.
6. Xu, Z. T. and J. Xu, "Design of dual-mode filters using stepped impedance resonators with stub loading," *2012 International Conference on Microwave and Millimeter Wave Technology (ICMMT)*, Vol. 4, 1–3, IEEE, 2012.
7. Goron, E., J.-P. Coupez, C. Person, Y. Toutain, H. Lattard, and F. Perrot, "Accessing to UMTS filtering specifications using new microstrip miniaturized loop-filters," *IEEE MTT-S Int. Microw. Symp. Dig.*, 1599–1602, Jun. 2003.
8. Konpang, J., "A compact diplexer using square open loop with stepped impedance resonators," *Asia-Pacific Microwave Conference*, 1–4, 2008.
9. Chuang, M.-L. and M.-T. Wu, "Microstrip diplexer design using common T-shaped resonator," *IEEE Microwave and Wireless Components Letters*, Vol. 21, No. 11, 583–585, 2011.
10. Guan, X., F. Yang, H. Liu, and L. Zhu, "Compact and high-isolation diplexer using dual-mode stub-loaded resonators," *IEEE Microwave and Wireless Components Letters*, Vol. 24, No. 6, 385–387, 2014.

11. Peng, H. S. and Y. C. Chiang, "Microstrip diplexer constructed with new types of dual-mode ring filters," *IEEE Microwave Wireless Compon. Lett.*, Vol. 25, No. 1, 7–9, 2015.
12. Yang, T., P.-L. Chi, and T. Itoh, "High isolation and compact diplexer using the hybrid resonators," *IEEE Microwave Wireless Compon. Lett.*, Vol. 20, No. 10, 551–553, 2010.
13. Guan, X., F. Yang, H. Liu, and L. Zhu, "Compact and high-isolation diplexer using dual-mode stub-loaded resonators," *IEEE Microwave Wireless Compon. Lett.*, Vol. 24, No. 6, 385–387, 2014.
14. Cheng, F., X. Q. Lin, Z. B. Zhu, L. Y. Wang, and Y. Fan, "High isolation diplexer using quarter-wavelength resonator filter," *Electron Lett.*, Vol. 48, No. 6, 330–331, 2012.
15. Xiao, J.-K., M. Zhu, Y. Li, L. Tian, and J.-G. Ma, "High selective microstrip bandpass filter and diplexer with mixed electromagnetic coupling," *IEEE Microwave Wireless Compon. Lett.*, Vol. 25, No. 12, 781–783, 2015.
16. Xu, J. X. and X. Y. Zhang, "Compact high-isolation LTCC diplexer using common stub-loaded resonator with controllable frequencies and bandwidths," *IEEE Transactions on Microwave Theory and Techniques*, Vol. 65, No. 11, 4636–4644, 2017.
17. Konpang, J. and N. Wattikornsirikul, "Four-port dual-mode diplexer with high signal isolation," *Active and Passive Electronic Components 2020*, 2020.
18. Keshavarz, S., R. Keshavarz, and A. Abdipour, "Compact active duplexer based on CSRR and interdigital loaded microstrip coupled lines for LTE application," *Progress In Electromagnetics Research C*, Vol. 109, 27–37, 2021.
19. Keshavarz, S., A. Abdipour, A. Mohammadi, and R. Keshavarz, "Design and implementation of low loss and compact microstrip triplexer using CSRR loaded coupled lines," *AEU — International Journal of Electronics and Communications*, Vol. 111, 152913, 2019.
20. Keshavarz, R., A. Mohammadi, and A. Abdipour, "A quad-band distributed amplifier with E-CRLH transmission line," *IEEE Transactions on Microwave Theory and Techniques*, Vol. 61, No. 12, 4188–4194, 2013.
21. Keshavarz, R. and N. Shariati, "Low profile metamaterial band-pass filter loaded with 4-turn complementary spiral resonator for WPT applications," *2020 27th IEEE International Conference on Electronics, Circuits and Systems (ICECS)*, 1–4, IEEE, 2020.
22. Keshavarz, R., Y. Miyanaga, M. Yamamoto, T. Hikage, and N. Shariati, "Metamaterial-inspired quad-band notch filter for LTE band receivers and WPT applications," *2020 XXXIIIrd General Assembly and Scientific Symposium of the International Union of Radio Science*, 1–4, IEEE, 2020.
23. Keshavarz, R., M. Movahhedi, and A. Hakimi, "A compact 0-dB coupled-line forward coupler by loading with shunt periodic stubs," *2010 Asia-Pacific Microwave Conference*, 1248–1251, IEEE, 2010.
24. Konpang, J. and N. Wattikornsirikul, "Dual-mode dual-band bandpass filter with high cutoff rejection by using asymmetrical transmission zeros technique," *Progress In Electromagnetics Research M*, Vol. 100, 225–236, 2021.